

Robustness of quantum critical pairing against disorder

Jian Kang* and Rafael M. Fernandes

School of Physics and Astronomy, University of Minnesota, Minneapolis, MN 55455, USA

Motivated by the remarkably robustness of many unconventional superconductors against disorder, we investigate the impact of weak impurity scattering on the onset of the pairing state mediated by quantum critical magnetic fluctuations. By expressing the Eliashberg equations in a functional form, we find that both the build-up of incoherent electronic spectral weight near the magnetic quantum phase transition, as well as the changes in the antiferromagnetic fluctuations caused by disorder, lead to a significant reduction in the suppression rate of T_c with disorder, as compared to extensions of the conventional theory of dirty superconductors. Our results shed new light on the understanding of unconventional superconductivity in correlated materials, where disorder is always present.

Elucidating the nature of unconventional superconductivity (SC) remains a major challenge in condensed matter physics. The fact that unconventional SC is found in proximity to a magnetic instability in many heavy-fermion [1, 2], organic [3, 4], cuprate [5], and iron-based compounds [6], led to the proposal that magnetic fluctuations promote the binding of the electrons in Cooper pairs, resulting in gap functions that change sign across the Brillouin zone (such as d -wave and s^{+-} -wave gaps) [7–20]. Indeed, in the phase diagram of high-temperature superconductors such as electron-doped cuprates and iron pnictides, the maximum value of T_c is observed very close to a putative antiferromagnetic (AFM) quantum critical point (QCP) [21–24], as shown in Fig. 1. Consequently, the possibility of pairing mediated by quantum critical fluctuations has been extensively investigated recently [25–33].

Experimentally, a major tool to probe unconventional SC has been the behavior of T_c with disorder [34]. In conventional superconductors displaying a s -wave gap, weak non-magnetic impurity scattering is known to be inconsequential to T_c [35], whereas magnetic impurities suppress T_c according to the Abrikosov-Gor'kov (AG) expression [36]. For a small pair-breaking scattering rate τ^{-1} , AG yields the universal suppression rate of T_c , $dT_c/d\tau^{-1} = -\pi/4$, confirmed experimentally [37]. Qualitatively, extensions of the AG theory to d -wave and s^{+-} superconductors reveal that non-magnetic impurities are in general pair-breaking. However, quantitatively, the experimentally observed suppression of T_c with disorder in cuprates and pnictides is rather small compared to the AG-based results [38–43]. Several scenarios have been proposed to reconcile this robustness of SC against disorder [44–53], including models advocating for a standard s -wave gap in the pnictides [54].

Therefore, elucidating how disorder affects AFM-mediated pairing beyond the AG paradigm is fundamental to advance our understanding of unconventional SC. This becomes particularly important since most unconventional SC are far from the clean regime. In this paper, we address the problem of disorder in a general spin-fermion model that describes SC promoted by quantum-

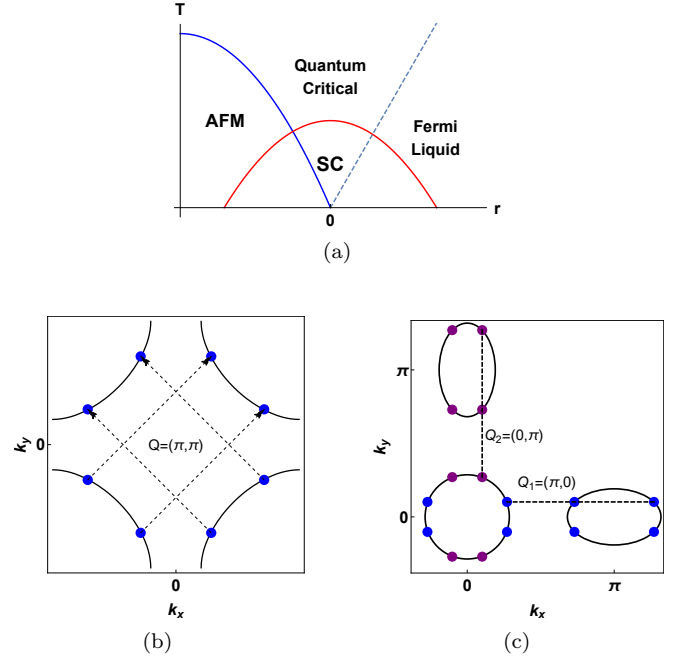


Figure 1. (a) Schematic phase diagram with the SC dome near the AFM quantum critical point. (b) and (c): Schematic Fermi surfaces of the cuprates and iron pnictides, respectively. Pairs of hot spots (blue or purple points) are connected by dashed lines, corresponding to the momentum $\mathbf{Q} = (\pi, \pi)$, for the cuprates, and $\mathbf{Q} = (\pi, 0)$ or $(0, \pi)$, for the pnictides. Spin fluctuations are peaked at these wave-vectors in the two materials.

critical AFM fluctuations, which can be applied to both cuprates and pnictides. Previously, Ref. [45] found a strikingly resilient SC state against the effects of disorder near an AFM-QCP. Here, instead of solving the coupled Eliashberg equations [55], we express them in a convenient functional form [9, 56–58] that allows us to compute directly $dT_c/d\tau^{-1}$ and gain invaluable insight on the different processes by which weak impurity scattering affects T_c . We find two effects absent in the conventional theory of dirty SC that cause a significant

reduction of the suppression rate $dT_c/d\tau^{-1}$ from the universal AG value. The first is the decrease of the electronic coherent spectral weight near the QCP, which effectively suppresses the reduction of the pairing vertex caused by pair-breaking scattering, in agreement with the general results from Ref. [45]. The second effect is the impact of disorder on the AFM fluctuations, a consequence of the fact that these bosonic excitations are collective electronic modes. In this case, while disorder suppresses the correlation length of the quantum critical fluctuations, it also renormalizes the electron-boson vertex, leading to an additional reduction of $dT_c/d\tau^{-1}$ with respect to the AG value. Our results offer a fresh perspective on the robustness of unconventional SC against disorder, lending support to the proposal that quantum critical pairing plays an important role in copper- and iron-based SC.

Our starting point is the low-energy spin-fermion model, in which electrons couple to a bosonic AFM order parameter ϕ_q , whose fluctuations are described by the magnetic susceptibility $\chi_b(q)$. Here, $q = (\mathbf{q}, \Omega_n)$ with momentum \mathbf{q} and bosonic Matsubara frequency $\Omega_n = 2n\pi T$. We focus on the electronic states $c_{\mathbf{k}\sigma}$ and $d_{\mathbf{k}\sigma} \equiv c_{\mathbf{k}+\mathbf{Q}\sigma}$ in the vicinities of a pair of hot spots, i.e. points of the Fermi surface connected by the AFM ordering vector \mathbf{Q} . The action is given by [26, 45]:

$$S = \int_k (-i\omega_n + \epsilon_c(\mathbf{k})) c_{\mathbf{k}\sigma}^\dagger c_{\mathbf{k}\sigma} + \int_k (-i\omega_n + \epsilon_d(\mathbf{k})) d_{\mathbf{k}\sigma}^\dagger d_{\mathbf{k}\sigma} + \lambda \int_{k,q} \phi_{-q} \cdot (c_{k,\alpha}^\dagger \sigma_{\alpha\beta} d_{k+q,\beta}) + \int_q \chi_b^{-1}(\mathbf{q}, \Omega_n) \phi_q \cdot \phi_{-q} \quad (1)$$

where $\int_k = T \sum_n \int \frac{d^d k}{(2\pi)^d}$, λ is the coupling constant, $\epsilon_d(\mathbf{k}) \equiv \epsilon_c(\mathbf{k} + \mathbf{Q})$, and $\omega_n = (2n+1)\pi T$ is the fermionic Matsubara frequency. Because the behavior of this action is dominated by the states near the hot spots [28], we linearize the spectrum near them, $\epsilon_c(\mathbf{k}) \approx \mathbf{v}_c \cdot \mathbf{k}$ and $\epsilon_d(\mathbf{k}) \approx \mathbf{v}_d \cdot \mathbf{k}$, where \mathbf{k} is measured with respect to the Fermi momentum. Thus, by focusing on a single pair of hot spots, this model can in principle be applied to either cuprates or pnictides. Indeed, as shown in Fig. 1, there are four pairs of hot spots in the typical Fermi surface of the cuprates (in which $\mathbf{Q} = (\pi, \pi)$) and eight for the iron pnictides (in which $\mathbf{Q} = (\pi, 0)$ or $(0, \pi)$). Hereafter, for simplicity, we consider the special case $|\mathbf{v}_c| = |\mathbf{v}_d|$, but the main results should remain valid otherwise.

For such a low-energy model, the magnetic susceptibility can be expanded as $\chi_b^{-1}(\mathbf{q}, \Omega_n) = \chi_0^{-1}(r_0 + q^2 + \Omega_n^2/v_b^2)$, where χ_0^{-1} is the magnetic energy scale determined by high-energy states, r_0 is the distance to the bare critical point, and v_b is the spin-wave velocity. The coupling to the electronic degrees of freedom, however, fundamentally changes this propagator by introducing Landau damping, i.e. the decay of magnetic excitations in electron-hole pairs. Within one-loop, the renormalized magnetic suscepti-

bility becomes $\chi^{-1} = \chi_b^{-1} - \Pi(\mathbf{q}, \Omega_n)$, where Π is the standard Lindhard function. Expanding it for small momentum and frequency, we find:

$$\chi(\mathbf{q}, \Omega_n) = \frac{\chi_0}{\xi^{-2} + q^2 + |\Omega_n|/\gamma}, \quad (2)$$

where $\xi^{-2} = r_0 - \chi_0 \Pi(0, 0)$ is the inverse squared correlation length, which vanishes at the QCP, and $\gamma^{-1} = \lambda^2 \chi_0 / (2\pi v_F^2 \sin \theta)$ is the Landau damping. Here, θ is the angle between \mathbf{v}_c and \mathbf{v}_d . To complete the model, we introduce the contributions from the small-momentum and large-momentum impurity potentials, u_0 and u_Q respectively: $S_{\text{imp}} = \int_{kk'} u_0 (c_{\mathbf{k}\sigma}^\dagger c_{\mathbf{k}'\sigma} + d_{\mathbf{k}\sigma}^\dagger d_{\mathbf{k}'\sigma}) + \int_{kk'} u_Q (c_{\mathbf{k}\sigma}^\dagger d_{\mathbf{k}'\sigma} + h.c.)$. For a point-like impurity, such as considered in Ref. [45], it follows that $u_0 = u_Q$.

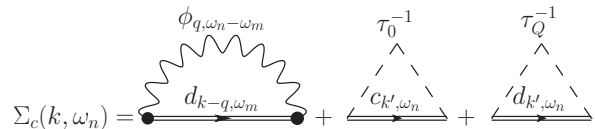


Figure 2. Feynman diagrams for the fermionic self-energy Σ , including the fermion-boson coupling and the disorder scattering.

Within the Eliashberg approach, the SC gap equations are obtained by evaluating the one-loop self-energy shown in Fig. 2. As shown in Ref. [26], the neglect of vertex corrections due to the bosonic propagator is justified in the $N \rightarrow \infty$ limit. Here, N is the number of hot spots, which plays the same role as the ratio between the ionic and electronic masses for the conventional electron-phonon SC problem. The normal component of the self-energy has a real part Σ' , which can be absorbed as a renormalization of the band dispersion, and an imaginary part Σ'' , which gives rise to a frequency-dependent fermionic coherent spectral weight Z_n^{-1} according to $Z_n = 1 - \Sigma''/\omega_n$. The anomalous component of the self-energy, W_n , is proportional to the frequency-dependent SC gap, $\Delta_n = W_n/Z_n$. Spin fluctuations promote attraction in the SC channel in which the gap changes sign from one hot spot to another, i.e. $W_n^c = -W_n^d \equiv W_n$, corresponding to either a d -wave gap or an s^{+-} gap, depending on the position of the hot spots in the Brillouin zone (see Fig. 1). The linearized coupled Eliashberg equations, valid at $T \gtrsim T_c$, become (see Supplementary Material (SM)):

$$Z_n = 1 + \frac{3\lambda^2 T}{2v_f \omega_n} \sum_m \text{sgn}(\omega_m) A(\omega_n - \omega_m) + \frac{(\tau_0^{-1} + \tau_Q^{-1})}{2|\omega_n|} \quad (3)$$

$$W_n = \frac{3\lambda^2 T}{2v_f} \sum_m \frac{W_m}{Z_m} A(\omega_n - \omega_m) + \frac{W_n (\tau_0^{-1} - \tau_Q^{-1})}{2|\omega_n| Z_n} \quad (4)$$

where $\tau_i^{-1} = 2\pi n_{\text{imp}} u_i^2 N_F$ are the impurity scattering rates and N_F is the density of states. The Born approximation is justified since we are interested in the limit of weak impurity scattering. The pairing interaction $A(\Omega_n)$ arises from the bosonic propagator:

$$A(\Omega_n) \approx \int \frac{dq_{\parallel}}{2\pi} \chi(q_{\parallel}, 0, \Omega_n) = \frac{\chi_0}{2\sqrt{\xi^{-2} + |\Omega_n|/\gamma}} \quad (5)$$

where the integration is restricted to momenta q_{\parallel} along the Fermi surface. Near the QCP, the contribution arising from the integration over the momenta q_{\perp} perpendicular to the Fermi surface is small for energies smaller than the cutoff $\Omega_c \sim v_f^2/\gamma$, which we employ hereby.

Our goal is to investigate how $dT_c/d\tau^{-1}$ deviates from the universal AG result, $(dT_c/d\tau^{-1})_{\text{AG}} = -\pi/4$. To gain insight into this problem, instead of directly solving the Eliashberg equations in the presence of disorder, we re-express them as a functional [9, 56–58]. In particular, after defining $\bar{\Delta}_n = TW_n/(Z_n|\omega_n|)$ and restricting the solution to even-frequency pairing, $W(-\omega_n) = W(\omega_n)$, solving the Eliashberg equations becomes equivalent to finding the zero eigenvalue η of $\hat{K}_{mn}\bar{\Delta}_n = \eta\bar{\Delta}_m$. Here, $\hat{K}_{mn} = -\delta_{mn}\hat{K}_{nn}^{(1)} + \sqrt{\frac{\Lambda}{T}}\hat{K}_{mn}^{(2)}$ with (see SM):

$$\hat{K}_{nn}^{(1)} = \frac{\tau_Q^{-1}}{T} + 2\pi \left(n + \frac{1}{2} \right) + \sqrt{\frac{\Lambda}{T}} \sum_{n'} \frac{\text{sgn}(\omega_{n'})}{\sqrt{|n - n'| + \frac{r}{T}}} \\ \hat{K}_{mn}^{(2)} = \left(|n - m| + \frac{r}{T} \right)^{-\frac{1}{2}} + \left(n + m + 1 + \frac{r}{T} \right)^{-\frac{1}{2}} \quad (6)$$

where m, n are non-negative integers, $r = \frac{\xi^{-2}\gamma}{2\pi}$ is the energy scale of the AFM fluctuations, and $\Lambda = \frac{9}{16}\lambda^2\chi_0 \sin\theta$ is an effective coupling constant. T_c is obtained when the largest eigenvalue η vanishes. These equations reduce to those studied in Ref. [45] when $\tau_0^{-1} = \tau_Q^{-1}$. The main advantage of this functional approach is that it allows us to study the impact of weak disorder on T_c without having to solve explicitly the disordered equations. This is accomplished by employing the Hellmann-Feynman theorem, $\frac{dT_c}{d\tau^{-1}} = -\left\langle \frac{d\hat{K}}{d\tau^{-1}} \right\rangle / \left\langle \frac{d\hat{K}}{dT_c} \right\rangle$, where $\langle \dots \rangle$ refers to an average with respect to the normalized eigenvector $\bar{\Delta}_n$. An immediate consequence of this expression is that, because only the large-momentum scattering rate τ_Q^{-1}

appears in the functional \hat{K} , T_c is insensitive to small-momentum scattering τ_0^{-1} – an extension of the Anderson theorem to sign-changing SC gaps.

To understand how T_c is affected by disorder in this model, we consider two limiting cases. First, we focus on the case where the system is far away from the QCP and the coupling constant is small, $r \gg \Omega_c \gg \Lambda$. The pairing interaction then becomes frequency-independent and small, $A(\Omega_n) \propto r^{-1/2}$, and the fermionic coherence factor can be approximated by $Z_n \approx 1$. Diagonalization of the matrix \hat{K} then yields the BCS-like expression $T_c \propto \Omega_c \exp\left(-\frac{1}{\pi}\sqrt{\frac{\Lambda}{r}}\right)$, and application of the Hellmann-Feynman theorem gives $dT_c/d\tau_Q^{-1} = -\pi/4$ (see SM). Therefore, far from the QCP, we recover the standard AG result for dirty superconductors.

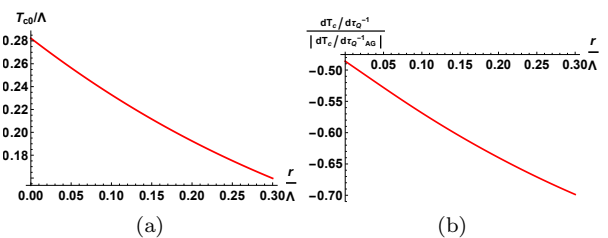


Figure 3. (a) SC transition temperature of the clean system (T_{c0}) as a function of the distance to the QCP, r , for $\Omega_c = 3\Lambda$. (b) Ratio between the suppression rate of T_c with pair-breaking scattering, $dT_c/d\tau_Q^{-1}$, and the AG absolute value $|dT_c/d\tau_Q^{-1}|_{\text{AG}} = \pi/4$, as function of r . In this calculation, only the coupling between disorder and fermionic states is considered.

The second limiting case corresponds to the system at the QCP, for which $r \propto \xi^{-2} = 0$. In this case, the pairing interaction is strongly frequency-dependent, $A(\Omega_n) \propto \Omega_n^{-1/2}$. From Eq. (3), we find that as $T \rightarrow 0$ the low-frequency coherent factor vanishes as $Z^{-1}(\omega \ll \Omega_c) \propto \omega^{1/2}$, a hallmark of non-Fermi liquid behavior. At the QCP, the SC eigenvalue problem can be solved even in the limit $\Omega_c \rightarrow \infty$, because the eigenvectors strongly decay as function of frequency, $\bar{\Delta}_{n \gg 1} \propto n^{-3/2}$. In this case, as shown in the SM, the solution of the eigenvalue problem yields the universal values $T_c \approx 0.5\Lambda$ and $dT_c/d\tau_Q^{-1} \approx -0.43$, i.e. the suppression rate of T_c is reduced with respect to the AG value. As discussed above, in our model Eq. (5) enforces a minimum cutoff in our problem, $\Omega_c \approx v_f^2/\gamma \sim \Lambda$. In this case, our numerical calculations show that both T_c and $-dT_c/d\tau_Q^{-1}$ increase and saturate as $\Omega_c \rightarrow \infty$, with $|dT_c/d\tau_Q^{-1}| \leq 0.43$.

Therefore, the two limiting cases suggest that proximity to the QCP promotes the robustness of T_c against pair-breaking disorder. To verify this property, in Fig 3 we plot T_c and $dT_c/d\tau_Q^{-1}$ as function of the distance to the QCP r , for a fixed cutoff $\Omega_c = 3\Lambda$. These results were obtained by diagonalizing Eq. (6) and apply-

ing Hellmann-Feynman theorem (see SM). As expected from the analysis above, T_c is continuously suppressed and $-dT_c/d\tau_Q^{-1}$ is continuously enhanced as the system moves away from the QCP. We checked that although the precise numbers depend on the ratio Ω_c/Λ , the general trend is robust, and $-dT_c/d\tau_Q^{-1}$ remains well below the AG universal value $\pi/4$. To understand this behavior, we note that the last term of the Eliashberg equation (4), proportional to τ_Q^{-1} , effectively reduces the pairing vertex to $\lambda \rightarrow \lambda / \left(1 + \frac{\tau_Q^{-1}}{2Z_n|\omega_n|}\right)$. Therefore, because at the QCP the fermionic coherent weight $Z^{-1} \propto \omega^{1/2}$ vanishes at the Fermi surface, the effect of disorder on the pairing vertex becomes less relevant at low frequencies, where the gap function is the largest. As the system moves away from the QCP, Z^{-1} enhances at the Fermi level, and disorder becomes more relevant.

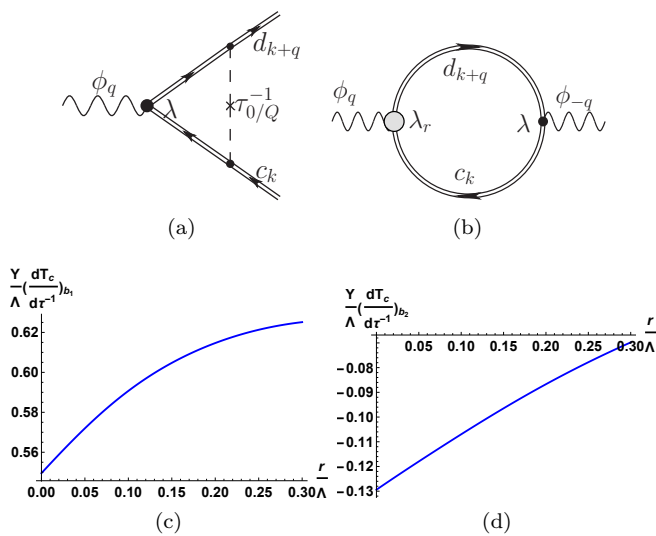


Figure 4. Dressing of the fermion-boson vertex (a) and of the bosonic self-energy (b) by disorder. The contribution from (a) enhances the fermionic coherent spectral weight, resulting in the enhancement of T_c by disorder (c). The contribution from (b) suppresses the magnetic correlation length, resulting in a suppression of T_c by disorder (d).

Our analysis so far, which agrees with the results from Ref. [45], has mirrored the standard AG approach for conventional dirty superconductors, with disorder impacting the fermionic degrees of freedom. The main difference between the conventional and unconventional SC cases, in this context, stems from the reduced coherent electronic spectral weight near the QCP. There is however another important difference between the two cases: while in the former the pairing interaction arises from an independent degree of freedom (phonons), in the latter it arises from the same electronic degrees of freedom (AFM fluctuations). This is manifested, for instance, by the renormalization of the bosonic AFM propagator by the Lindhard function, $\chi_0^{-1} = \chi^{-1} - \Pi$. Therefore, the cou-

pling between fermions and the impurity potential also affects the bosonic propagator [59, 60], causing additional contributions to $dT_c/d\tau_Q^{-1}$.

Within our functional approach to the Eliashberg equations, including this effect is straightforward within linear order in τ^{-1} . In particular, the two processes through which the bosonic degrees of freedom are affected by disorder scattering are shown in the diagrams of Fig. 4(a) and 4(b). The first corresponds to a renormalization of the electron-boson coupling, which becomes $\tilde{\lambda}_{nm} = \lambda \left(1 + \frac{\text{sgn}(\omega_m \omega_n)}{2\tau\Upsilon}\right)^{-1}$ [61], where $\Upsilon = 4\pi N_F v_F^2 \sin \theta \sim E_F$ and $\tau^{-1} = \tau_0^{-1} + \tau_Q^{-1}$ is the total scattering rate. The second corresponds to a renormalization of the bosonic propagator in Eq. (2) via the Lindhard function. We find that while the Landau damping γ depends only quadratically on the scattering rate, the correlation length ξ is reduced by impurities, such that $dr/d\tau^{-1} = \Omega_c/(4\pi\Upsilon)$. This last result is consistent with previous works that found a reduction of the magnetic order parameter with disorder in itinerant AFM systems [62, 63]. Note that in contrast to the previous contributions to $dT_c/d\tau_Q^{-1}$, $dr/d\tau^{-1}$ depends on the upper cutoff, implying that high-energy states are relevant for this process.

Using Hellmann-Feynman theorem, we can separate the three different contributions to the reduction of T_c with impurity scattering, $\frac{dT_c}{d\tau^{-1}} = \left(\frac{dT_c}{d\tau^{-1}}\right)_f + \left(\frac{dT_c}{d\tau^{-1}}\right)_{b,1} + \left(\frac{dT_c}{d\tau^{-1}}\right)_{b,2}$. Here, $\left(\frac{dT_c}{d\tau^{-1}}\right)_f$ denotes the pair-breaking effect arising from the coupling between the electrons and the large-momentum impurity potential, $\left(\frac{dT_c}{d\tau^{-1}}\right)_{b,1}$ corresponds to the dressing of the electron-boson vertex by impurities, and $\left(\frac{dT_c}{d\tau^{-1}}\right)_{b,2}$ corresponds to the dressing of the bosonic propagator by impurities. As analyzed above in Fig. 3, $\left(\frac{dT_c}{d\tau^{-1}}\right)_f$ is always negative albeit reduced with respect to the AG value near the QCP. The $\left(\frac{dT_c}{d\tau^{-1}}\right)_{b,2}$ contribution is straightforward to obtain: because $r \propto \xi^{-2}$ is enhanced by disorder, the system behaves as it moves away from the QCP, which effectively reduces T_c , according to the behavior found previously in Fig. 3. Our numerical evaluation reveals indeed that $\left(\frac{dT_c}{d\tau^{-1}}\right)_{b,2} < 0$ near the QCP, as shown in Fig. 4(d).

Numerical computation of the $\left(\frac{dT_c}{d\tau^{-1}}\right)_{b,1}$ contribution, however, shows that surprisingly $\left(\frac{dT_c}{d\tau^{-1}}\right)_{b,1} > 0$ close to the QCP, as plotted in Fig. 4(c). This unexpected result can be understood by analyzing the expression for the coherent spectral weight Z_n^{-1} , Eq. (3), in the presence of the renormalized electron-boson coupling $\tilde{\lambda}$ (and in the absence of other impurity terms). At the QCP, we find that at low frequencies, $\omega \ll \Lambda_c$, Z_n is effectively reduced by this vertex renormalization, $dZ/d\tau^{-1} \propto -\Upsilon/\omega$. Consequently, because Z_n appears in the denominator of the pairing kernel in the gap equation (4), the SC transition temperature is enhanced by this effect.

Having established the different contributions to $dT_c/d\tau^{-1}$, we discuss their relative magnitudes. Our analytical approximations, presented in details in the SM, combined with the numerical results, show that at the QCP the two effects arising from the coupling of the bosons to the impurity potential behave as $|\frac{dT_c}{d\tau^{-1}}|_{b,2} \sim \frac{0.04}{\sin\theta} |\frac{dT_c}{d\tau^{-1}}|_{b,1}$. Therefore, unless the system is very close to perfect nesting ($\theta = 0$), the positive contribution $(\frac{dT_c}{d\tau^{-1}})_{b,1}$ overcomes the negative contribution $(\frac{dT_c}{d\tau^{-1}})_{b,2}$. Consequently, the suppression rate of T_c enforced by the direct coupling of the fermions to the impurity potential $(dT_c/d\tau^{-1})_f$ is reduced even more as compared to the AG value. As shown in Fig. 4, $|\frac{dT_c}{d\tau^{-1}}|_{b,1} \sim \frac{\lambda^2\chi_0}{E_F} |\frac{dT_c}{d\tau^{-1}}|_f$, implying that this additional enhancement of T_c is generally smaller than the reduction promoted by pair-breaking effects. Equivalently, within an expansion in the number of hot spots N , this additional contribution acquires a prefactor of $1/\sqrt{N}$.

In summary, we have shown that the suppression of T_c by weak disorder in an AFM quantum critical SC is significantly reduced compared to the universal value obtained from the AG theory of conventional dirty SC. Our work highlights the importance of the incoherent electronic spectral weight and of the feedback of the electronic states on the pairing interaction to describe the properties of this unconventional pairing state. Qualitatively, our results agree with several experimental observations in cuprates and pnictides reporting a robust SC state against disorder. Extensions of this promising framework to include higher-order contributions from the impurity scattering would be desirable to achieve more quantitative comparisons with experiments, such as the critical value of the impurity scattering that destroys the quantum critical SC state.

We thank A. Chubukov, A. Millis, J. Schmalian, X. Wang, and Y. Wang for fruitful discussions. This work was supported by the U.S. Department of Energy, Office of Science, Basic Energy Sciences, under award number DE-SC0012336.

* jkang@umn.edu

- [1] F. Steglich, J. Aarts, C.D. Bredl, W. Lieke, D. Meschede, W. Franz, and H. Schafer, Phys. Rev. Lett. **43**, 1892 (1979).
- [2] G.R. Stewart, Z. Fisk, J.O. Willis, and J.L. Smith, Phys. Rev. Lett. **52**, 679 (1984).
- [3] D. Jerome, A. Mazaud, M. Ribault, and K. Bechgaard. J. Phys. (Paris) Lett. **41** L95, 1980.
- [4] S. M. De Soto, C. P. Slichter, A. M. Kini, H. H. Wang, U. Geiser, and J. M. Williams, Phys. Rev. B **52**, 10364 (1995).
- [5] J. G. Bednorz and K. A. Muller, Z. Phys. B **64**, 189 (1986).
- [6] Y. Kamihara, T. Watanabe, M. Hirano, and H. Hosono,

- J. Am. Chem. Soc. **130**, 3296 (2008).
- [7] J.E. Hirsch, Phys. Rev. Lett. **54**, 1317 (1985).
- [8] K. Miyake, S. Schmitt-Rink, and C.M.Varma, Phys. Rev. B **34**, 6554 (1986).
- [9] A.J. Millis, S. Sachdev, and C.M.Varma, Phys. Rev. B **37**, 4975 (1988).
- [10] D.J. Scalapino, E. Loh, Jr. and J.E. Hirsch, Phys. Rev. B **34**, 8190 (1986).
- [11] D.A. Wollman, D.J.Van Harlingen, W.C. Lee, D.M. Ginsberg, and A.J. Leggett, Phys. Rev. Lett. **71**, 2134 (1993).
- [12] D. J Van Harlingen, Physica C **282-287**, 128 (1997).
- [13] C.C. Tsuei, J.R. Kirtley, C.C. Chi, Lock See Yu-Jahnes, A. Gupta, T. Shaw, J.Z. Sun, and M.B. Ketchen, Phys. Rev. Lett. **73**, 593 (1994).
- [14] P. Monthoux and D. Pines, Phys. Rev. Lett. **69**, 961 (1992).
- [15] P. Monthoux, D. Pines, and G. G. Lonzarich, Nature, **450**, 1177 (2007).
- [16] I. I. Mazin, D. J. Singh, M. D. Johannes, and M. H. Du, Phys. Rev. Lett. **101**, 057003 (2008).
- [17] K. Kuroki, S. Onari, R. Arita, H. Usui, Y. Tanaka, H. Kontani, and H. Aoki. Phys. Rev. Lett. **101**, 087004 (2008).
- [18] P.J. Hirschfeld, M. M. Korshunov, and I. I. Mazin, Rep. Prog. Phys. **74**, 124508 (2011).
- [19] D. J. Scalapino, Rev. Mod. Phys. **84**, 1383 (2012).
- [20] A. V. Chubukov, Annu. Rev. Cond. Mat. Phys. **3**, 57 (2012).
- [21] T. Valla, A. V. Fedorov, P. D. Johnson, B. O. Wells, S. L. Hulbert, Q. Li, G. D. Gu, and N. Koshizuka, Science **285** 2110 (1999).
- [22] S. Jiang, H. Xing, G. Xuan, C. Wang, Z. Ren, C. Feng, J. Dai, Z. Xu and G. Cao, Journal of Physics: Condensed Matter **21**, 382203 (2009).
- [23] T. Shibauchi, A. Carrington, and Y. Matsuda, Annu. Rev. Condens. Matter Phys. **5**, 113 (2014).
- [24] S. Sachdev, *Quantum Phase Transitions* (Cambridge University Press, Cambridge, England, 2001).
- [25] A. Abanov, A.V. Chubukov and A.M. Finkel'stein, Europhys. Lett. **54**, 488 (1999).
- [26] A. Abanov, A. V. Chubukov, and J. Schmalian. Adv. Phys. **52**, 119 (2003).
- [27] M. A. Metlitski, and S. Sachdev, Phys. Rev. B **82**, 075127 (2010); Phys. Rev. B **82**, 075128 (2010).
- [28] E. Berg, M. A. Metlitski, and S. Sachdev, Science **338**, 1606 (2012).
- [29] M. A. Metlitski, D. F. Mross, S. Sachdev, and T. Senthil, Phys. Rev. B **91**, 115111 (2015).
- [30] J.-H. She, B. J. Overbosch, Y.-W. Sun, Y. Liu, K. E. Schalm, J. A. Mydosh, and J. Zaanen, Phys. Rev. B **84**, 144527 (2011).
- [31] S. Raghu, G. Torroba, and H. Wang, arXiv:1507.06652.
- [32] Y. Schattner, S. Lederer, S. A. Kivelson, and E. Berg, arXiv:1511.03282.
- [33] K. B. Efetov, H. Meier, and C. Pépin, Nat. Phys. **9**, 442 (2013).
- [34] A. V. Balatsky, I. Vekhter, and J.-X. Zhu, Rev. Mod. Phys. **78**, 373 (2006).
- [35] P. W. Anderson, J. Phys. Chem. Solids **11**, 26 (1959).
- [36] A. A. Abrikosov and L. P. Gor'kov, Sov. Phys. JET **12**, 1243 (1961).
- [37] M. A. Wolf and F. Reif, Phys. Rev. **137**, A557 (1965).
- [38] S. K. Tolpygo, J.-Y. Lin, M. Gurvitch, S. Y. Hou, and J.

- M. Phillips, Phys. Rev. B **53**, 12454 (1996).
- [39] K. Kirshenbaum, S. R. Saha, S. Ziemak, T. Drye, and J. Paglione, Phys. Rev. B **86**, 140505 (2012).
- [40] H. Alloul, J. Bobroff, M. Gabay, and P. J. Hirschfeld, Rev. Mod. Phys. **81**, 45 (2009).
- [41] K. Fujita, T. Noda, K. M. Kojima, H. Eisaki, and S. Uchida, Phys. Rev. Lett. **95**, 097006 (2005).
- [42] Y. Nakajima, T. Taen, Y. Tsuchiya, T. Tamegai, H. Kitamura, and T. Murakami, Phys. Rev. B **82**, 220504 (2010).
- [43] F. Rullier-Albenque, H. Alloul, and R. Tourbot, Phys. Rev. Lett. **91**, 047001 (2003).
- [44] A. F. Kemper, D. G. S. P. Doluweera, T. A. Maier, M. Jarrell, P. J. Hirschfeld, and H-P. Cheng, Phys. Rev. B **79**, 104502 (2009).
- [45] A. B. Vorontsov, Ar. Abanov, M. G. Vavilov, and A. V. Chubukov, Phys. Rev. B **81**, 012508 (2010).
- [46] Y. Wang, A. Kreisel, P. J. Hirschfeld, and V. Mishra, Phys. Rev. B **87**, 094504 (2013).
- [47] Y. Yamakawa, S. Onari, and H. Kontani, Phys. Rev. B **87**, 195121 (2013).
- [48] H. Chen, Y.-Y. Tai, C. S. Ting, M. J. Graf, J. Dai, J.-X. Zhu, Phys. Rev. B **88**, 184509 (2013).
- [49] M. S. Scheurer, M. Hoyer, J. Schmalian, Phys. Rev. B **92**, 014518 (2015).
- [50] A. Garg, M. Randeria, and N. Trivedi, Nature Physics **4**, 762 (2008).
- [51] R. J. Radtke, K. Levin, H.-B. Schuttler, and M. R. Norman, Phys. Rev. B **48**, 653 (1993).
- [52] M. Franz, C. Kallin, A. J. Berlinsky, and M. I. Salkola, Phys. Rev. B **56**, 7882 (1997).
- [53] S. Tang, V. Dobrosavljevic, and E. Miranda, arXiv:1510.08152.
- [54] S. Onari and H. Kontani, Phys. Rev. Lett. **103**, 177001 (2009).
- [55] G. M. Eliashberg, Sov. Phys. JETP **11**, 696 (1960); Sov. Phys. JETP **16**, 780 (1963).
- [56] D. J. Bergmann and D. Rainer, Z. Phys. **263**, 59 (1973).
- [57] R. M. Fernandes and A. J. Millis, Phys. Rev. Lett. **110**, 117004 (2013).
- [58] K. Levin and O. T. Valls, Phys. Rev. B, **17**, 191 (1978).
- [59] I. Martin, D. Podolsky, and S. A. Kivelson, Phys. Rev. B **72**, 060502(R) (2005).
- [60] A. T. Romer, S. Graser, T. S. Nunner, P. J. Hirschfeld, and B. M. Andersen, Phys. Rev. B **86**, 054507 (2012).
- [61] S. V. Syzranov and J. Schmalian, Phys. Rev. Lett. **109**, 156403 (2012).
- [62] R. M. Fernandes, M. G. Vavilov, and A. V. Chubukov, Phys. Rev. B **85**, 140512(R) (2012).
- [63] S. Liang, C. B. Bishop, A. Moreo, and E. Dagotto, Phys. Rev. B **92**, 104512 (2015).

Supplementary for “Robustness of quantum critical pairing against disorder”

I. ELIASHBERG EQUATIONS FOR THE SPIN-FERMION MODEL

In this section, we give a detailed derivation of the Eliashberg equations for the two-dimensional spin-fermion model. In the SC phase, the fermionic self energy has both normal and anomalous components in the Nambu spinor representation [S9]:

$$\Sigma(i\omega_n, \mathbf{k}) = i\omega_n(1 - Z_n)\sigma_0 + \zeta\sigma_3 + W_n\sigma_1 ,$$

where σ_i are Pauli matrices. In principle, both Z_n and W_n depend on the momentum \mathbf{k} . In our approach, where pairs of hot spots are considered, the momentum dependence is neglected and only the frequency dependence is considered. The fermionic Green’s function is given by:

$$G^{-1}(i\omega_n, \mathbf{k}) = i\omega_n Z_n - \epsilon\sigma_3 - W_n\sigma_1 \implies G(i\omega_n, \mathbf{k}) = -\frac{i\omega_n Z_n + \epsilon\sigma_3 + W_n\sigma_1}{(Z_n\omega_n)^2 + \epsilon^2 + W_n^2}$$

where we absorbed the real-part of the normal self-energy ζ in the electronic dispersion ϵ . The low-energy bosonic propagator has diffusive dynamics due to Landau damping:

$$\chi(i\Omega_n, \mathbf{q} + \mathbf{Q}) = \frac{\chi_0}{\xi^{-2} + \mathbf{q}^2 + |\Omega_n|/\gamma} . \quad (\text{S1})$$

By computing the one-loop self-energy in Fig. 2, the linearized Eliashberg equations ($T = T_c$) in the presence of disorder can be written as

$$i\omega_n(1 - Z_{n,c}(\mathbf{k})) = 3\lambda^2 T \sum_m \int \frac{d^2q}{(2\pi)^2} \frac{\chi_0}{\xi^{-2} + q^2 + |\omega_n - \omega_m|/\gamma} \frac{-i\omega_m Z_{m,d}}{(\omega_m Z_{m,d})^2 + \epsilon_d^2(\mathbf{k} - \mathbf{q})} - i \frac{\text{sgn}(\omega_n)}{2\tau} \quad (\text{S2})$$

$$W_{n,c}(\mathbf{k}) = T \sum_m \int \frac{d^2q}{(2\pi)^2} \frac{-3\lambda^2 \chi_0}{\xi^{-2} + q^2 + \frac{|\omega_n - \omega_m|}{\gamma}} \frac{W_{m,d}}{(\omega_m Z_{m,d})^2 + \epsilon_d^2(\mathbf{k} - \mathbf{q})} + \frac{(2\tau_0)^{-1} W_{n,c}}{|\omega_n| Z_{n,c}} + \frac{(2\tau_Q)^{-1} W_{n,d}}{|\omega_n| Z_{n,d}} \quad (\text{S3})$$

The subscript c, d refer to the fermionic states around the two hot spots. The equations for $Z_{n,d}$ and $W_{n,d}$ assume similar forms. The total impurity scattering rate is given by $\tau^{-1} = \tau_0^{-1} + \tau_Q^{-1}$, where τ_0^{-1} is the small-momentum scattering rate and τ_Q^{-1} is the large-momentum scattering rate. Linearizing the fermionic dispersion near the hot spots, we obtain

$$\epsilon_c(\mathbf{k}) \approx \mathbf{v}_c \cdot \mathbf{k}, \quad \epsilon_d(\mathbf{k}) \approx \mathbf{v}_d \cdot \mathbf{k}.$$

where \mathbf{k} is measured relative to the hot spots. Both Eqs. (S2) and (S3) contain the two-dimensional integral over momenta q_{\parallel} and q_{\perp} , i.e. the components of \mathbf{q} parallel and perpendicular to the Fermi surface. Focusing at the hot spot ($\mathbf{k} = 0$), we have

$$\begin{aligned} A(\omega_n - \omega_m) &= \int \frac{d^2q}{(2\pi)^2} \frac{\chi_0}{\xi^{-2} + q^2 + |\omega_n - \omega_m|/\gamma} \frac{-i\omega_m Z_{m,d}}{(\omega_m Z_{m,d})^2 + \epsilon_d^2(\mathbf{q})} \\ &= \frac{\chi_0}{2} \int \frac{dq_{\perp}}{(2\pi)} \frac{1}{\sqrt{\xi^{-2} + q_{\perp}^2 + |\omega_n - \omega_m|/\gamma}} \frac{-i\omega_m Z_{m,d}}{(\omega_m Z_{m,d})^2 + (v_f q_{\perp})^2} \\ &\approx \frac{\chi_0}{4v_f} \frac{-i\text{sgn}(\omega_m)}{\sqrt{\xi^{-2} + |\omega_n - \omega_m|/\gamma}}. \end{aligned} \quad (\text{S4})$$

where, in the last step, we considered that:

$$\xi^{-2} + |\omega_n - \omega_m|/\gamma \gg \left(\frac{\omega_m Z_m}{v_f} \right)^2 \quad (\text{S5})$$

which naturally establishes a cutoff:

$$\Omega_c = \max\left(\frac{v_f^2}{\gamma}, \frac{v_f}{\xi}\right) = \max\left(\frac{8\Lambda}{9\pi \sin^2 \theta}, \frac{4\sqrt{r\Lambda}}{3 \sin \theta}\right) \quad (\text{S6})$$

Therefore, the Eliashberg equations are given by:

$$Z_{n,c} = 1 + \frac{\sqrt{\Lambda/T}}{2\pi(n+1/2)} \sum_m \frac{\text{sgn}(\omega_m)}{\sqrt{|n-m|+r/T}} + \frac{1}{2\tau|\omega_n|} \quad (\text{S7})$$

$$W_{n,c} = -\sqrt{\frac{\Lambda}{T}} \sum_m \frac{W_{n,d}}{Z_{m,d}|m+1/2|} \frac{1}{\sqrt{|\omega_n - \omega_m| + r/T}} + \frac{W_{n,c}}{2\tau_0|\omega_n|Z_{n,c}} + \frac{W_{n,d}}{2\tau_Q|\omega_n|Z_{n,d}} \quad (\text{S8})$$

Similar equations hold for the fermionic states around the hot spot d . Assuming that $|\mathbf{v}_c| = |\mathbf{v}_d|$, $Z_{n,c} = Z_{n,d} = Z_n$ and $W_{n,c} = -W_{n,d} = W_n$. In addition, $Z(\omega_n) = Z(-\omega_n)$, and we focus on even-pairing SC solutions, $W(\omega_n) = W(-\omega_n)$. As a result, the Eliashberg equations become

$$Z_{n \geq 0} = 1 + \frac{\sqrt{\Lambda/T}}{2\pi(n+1/2)} \sum_m \frac{\text{sgn}(\omega_m)}{\sqrt{|n-m|+r/T}} + \frac{1}{2\tau|\omega_n|} \quad (\text{S9})$$

$$W_n = \sqrt{\frac{\Lambda}{T}} \sum_m \frac{W_m}{2\pi|m+1/2|Z_m} \frac{1}{\sqrt{|n-m|+r/T}} + \frac{W_n}{2\tau_0|\omega_n|Z_n} - \frac{W_n}{2\tau_Q|\omega_n|Z_n} \quad (\text{S10})$$

When the high energy cutoff $\Omega_c \rightarrow \infty$, we note that the summation in Eq.(S9) can be expressed by the Hurwitz zeta function,

$$Z_{n \geq 0} = 1 + \frac{\sqrt{\Lambda/T}}{2\pi(n+1/2)} \left\{ 2 \left[\zeta\left(\frac{1}{2}, 1 + \frac{r}{T}\right) - \zeta\left(\frac{1}{2}, n+1 + \frac{r}{T}\right) \right] + \sqrt{\frac{T}{r}} \right\} + \frac{1}{2\tau|\omega_n|}$$

Defining $\bar{\Delta}_n = W_n/(2\pi Z_n |n+1/2|)$, the gap equation can be written as

$$\sqrt{\frac{\Lambda}{T}} \sum_m \frac{\bar{\Delta}_m}{\sqrt{|n-m|+r/T}} + \left(\frac{1}{2\tau_0 T} - \frac{1}{2\tau_Q T} - 2\pi \left| n + \frac{1}{2} \right| Z_n \right) \bar{\Delta}_n = 0 \quad (\text{S11})$$

or, equivalently, as the matrix equation $\sum \hat{K}_{mn} \bar{\Delta}_m = 0$. Thus, T_c is obtained by the requirement that the largest eigenvalue of \hat{K} vanishes. Restricting the matrix indices to be non-negative, we have

$$\hat{K}_{mn} = \frac{\sqrt{\Lambda/T}}{\sqrt{|n-m|+r/T}} + \frac{\sqrt{\Lambda/T}}{\sqrt{n+m+1+r/T}} + \left(\frac{1}{2\tau_0 T} - \frac{1}{2\tau_Q T} - 2\pi \left| n + \frac{1}{2} \right| Z_n \right) \delta_{mn} \quad (\text{S12})$$

with the size of the matrix $N_c = \Omega_c/(2\pi T)$. Substituting the expression for Z_n then yields the final result:

$$\hat{K}_{m \neq n} = \sqrt{\frac{\Lambda}{T}} \left(\frac{1}{\sqrt{|n-m|+r/T}} + \frac{1}{\sqrt{n+m+1+r/T}} \right) \quad (\text{S13})$$

$$\hat{K}_{nn} = \frac{2\sqrt{\Lambda/T}}{\sqrt{2n+1+r/T}} - 2\pi \left(n + \frac{1}{2} \right) - \sqrt{\frac{\Lambda}{T}} \sum_{\substack{n' \neq n \\ n'=0}}^{N_c} \left(\frac{1}{\sqrt{|n-n'|+r/T}} - \frac{1}{\sqrt{n+n'+1+r/T}} \right) - \frac{1}{\tau_Q T}, \quad (\text{S14})$$

II. SOLUTIONS OF THE CLEAN ELIASHBERG EQUATIONS IN LIMITING CASES

Although in general the clean Eliashberg equations can only be solved numerically, two limiting cases can be treated analytically.

A. BCS limit

The BCS limit is achieved when the system is far from the QCP, $r \gg \Omega_c \gg \Lambda$. In this case, the bosonic spectral function in Eq. (S4) becomes frequency independent and $Z_n \approx 1$, according to Eq. S5. In this limit, Eq. (S11) becomes

$$K_{mn} \approx 2\sqrt{\frac{\Lambda}{r}} - \pi(2n+1)\delta_{mn} \quad \Longrightarrow \quad \bar{\Delta}_{n \geq 0} = \frac{2}{\pi(2n+1)} \sqrt{\frac{\Lambda}{r}} \sum_{m \leq \frac{\Omega_c}{2\pi T}} \bar{\Delta}_m \quad (\text{S15})$$

Defining the quantity $c = \sum_m \bar{\Delta}_m$, we obtain the self-consistent equation:

$$c = \frac{c}{\pi} \sqrt{\frac{\Lambda}{r}} \sum_{n \leq \Omega_c/(2\pi T)} \frac{1}{n+1/2} = \frac{c}{\pi} \sqrt{\frac{\Lambda}{r}} \left[\psi \left(\frac{\Omega_c}{2\pi T} - \frac{1}{2} \right) - \psi \left(\frac{1}{2} \right) \right] \quad \Longrightarrow \quad T_c \approx \frac{\Omega_c}{2\pi} \exp \left[-\pi \sqrt{\frac{r}{\Lambda}} - \psi \left(\frac{1}{2} \right) \right]$$

which agrees with the BCS expression. Here, $\psi(x)$ is the digamma function.

B. Quantum Critical Point

We first explain how the high-energy cutoff is set in our calculation. In the previous subsection discussing the BCS limit, we set a hard cutoff $N_c = \Omega_c/(2\pi T)$ in the Matsubara sum. Although this procedure does not affect the behavior of T_c in the limit of $\Omega_c \gg T_c$, it will make T_c behave discontinuously as Ω_c and r decrease. To avoid such a discontinuity, we set instead a soft cutoff in the Matsubara sum by including an appropriate continuous function $f(\omega_n)$ that is strongly suppressed above Ω_c and nearly 1 below Ω_c . Specifically, we change the bosonic propagator to:

$$\frac{1}{|\omega_n - \omega_m|/\gamma + \mathbf{q}^2 + \xi^{-2}} \rightarrow \frac{f(\omega_n)f(\omega_m)}{|\omega_n - \omega_m|/\gamma + \mathbf{q}^2 + \xi^{-2}} \quad \text{with} \quad f(\omega) = \left[\exp \left(\frac{|\omega| - \Omega_c}{\Lambda_d} \right) + 1 \right]^{-1}$$

where $\Lambda_d = 0$ gives the hard energy cutoff. As we can see, when $|\omega| \ll \Omega_c$, $f(\omega) \approx 1$, and when $|\omega| \gg \Omega_c$, $f(\omega) \approx 0$. In our calculation, Λ_d is set to be $\Lambda_d = \max(0.1\Lambda, 0.3\Omega_c)$. The matrix \hat{K} becomes

$$\begin{aligned}
f_{n \geq 0} &= f(\pi(2n+1)T) \\
\hat{K}_{m \neq n} &= f_m f_n \sqrt{\frac{\Lambda}{T}} \left(\frac{1}{\sqrt{|n-m|+r/T}} + \frac{1}{\sqrt{n+m+1+r/T}} \right) \\
\hat{K}_{nn} &= f_n^2 \sqrt{\frac{\Lambda}{(2n+1)T+r}} - \pi(2n+1) - f_n \sqrt{\frac{\Lambda}{T}} \sum_{m \neq n} \frac{\text{sgn}(\omega_m) f_m}{\sqrt{|n-m|+r/T}} - \frac{1}{\tau_Q T} \\
&= 2f_n^2 \sqrt{\frac{\Lambda}{(2n+1)T+r}} - \pi(2n+1) - f_n \sqrt{\frac{\Lambda}{T}} \sum_{\substack{n' \neq n \\ n'=0}}^{N_c} f_m \left(\frac{1}{\sqrt{|n-n'|+r/T}} - \frac{1}{\sqrt{n+n'+1+r/T}} \right) - \frac{1}{\tau_Q T}
\end{aligned} \tag{S16}$$

We emphasize that none of our results qualitatively change for $\Lambda_d = 0$ or Λ_d small. At the QCP, $r = 0$, yielding:

$$\begin{aligned}
K_{m \neq n} &= f_m f_n \sqrt{\frac{\Lambda}{T}} \left(\frac{1}{\sqrt{|n-m|}} + \frac{1}{\sqrt{n+m+1}} \right) \\
K_{nn} &= \sqrt{\frac{\Lambda}{T}} \frac{2f_n^2}{\sqrt{2n+1}} - \pi(2n+1) - f_n \sqrt{\frac{\Lambda}{T}} \sum_{\substack{n' \neq n \\ n'=0}}^{N_c} f_m \left(\frac{1}{\sqrt{|n-n'|}} - \frac{1}{\sqrt{n+n'+1}} \right) - \frac{1}{\tau_Q T}
\end{aligned} \tag{S18}$$

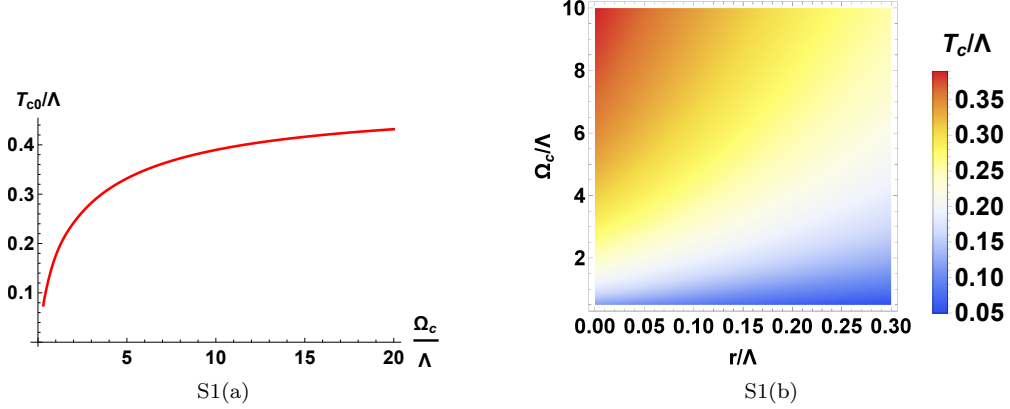


Figure S1. (a) T_{c0} (in the clean limit) as function of the high-energy cutoff Ω_c when the system is at QCP ($r = 0$). (b) T_{c0} as a function of r and Ω_c .

As show in Fig. S1, by numerically computing the eigenvalue of this matrix in the clean limit ($\tau_Q^{-1} = 0$), T_c is generally suppressed away from the QCP for a fixed value of Ω_c . At the QCP ($r = 0$), although T_c changes with the cutoff Ω_c , it is interesting to study the case $\Omega_c \rightarrow \infty$. In this limit, $f(\omega) \rightarrow 1$, and the \hat{K} matrix becomes

$$\hat{K}_{nn} = \frac{\sqrt{\Lambda/T}}{\sqrt{2n+1}} - \pi(2n+1) - 2\sqrt{\frac{\Lambda}{T}} \left[\zeta\left(\frac{1}{2}, 1\right) - \zeta\left(\frac{1}{2}, n+1\right) \right] \quad \hat{K}_{m \neq n} = \sqrt{\frac{\Lambda}{T}} \left(\frac{1}{\sqrt{|n-m|}} + \frac{1}{\sqrt{n+m+1}} \right).$$

where $\zeta\left(\frac{1}{2}, x\right)$ is the Hurwitz zeta function. Clearly, the only free parameter is the combination $\frac{\Lambda}{T_c}$. By numerically diagonalizing the matrix, we find $T_c \approx 0.5\Lambda$. Analysis of the eigenvalue problem for large frequencies reveal that $\bar{\Delta}_n \propto n^{-3/2}$, which ensures that one can safely take $\Omega_c \rightarrow \infty$. This is to be contrasted with the BCS case, in which $\bar{\Delta}_n \propto n^{-1}$, implying that the sum does not converge and a cutoff is needed.

III. COUPLING BETWEEN DISORDER AND FERMIONS

In this section we present the expressions for suppression rate of T_c , $dT_c/d\tau^{-1}$, due to the direct coupling between disorder and fermions. Using Hellmann-Feynman theorem, we have:

$$\left(\frac{dT_c}{d\tau^{-1}}\right)_{\tau^{-1}=0} = - \left(\frac{\partial\eta}{\partial\tau^{-1}}\right)_{T=T_{c_0}} \left(\frac{\partial\eta}{\partial T}\right)_{\tau^{-1}=0}^{-1},$$

where η is the largest eigenvalue of the matrix \hat{K} and:

$$\frac{\partial\eta}{\partial\tau^{-1}} = \left\langle \frac{\partial\hat{K}}{\partial\tau^{-1}} \right\rangle, \quad \text{and} \quad \frac{\partial\eta}{\partial T} = \left\langle \frac{\partial\hat{K}}{\partial T} \right\rangle.$$

Here, $\langle \hat{O} \rangle$ means the average value of \hat{O} with respect to the eigenvector of \hat{K} . From Eqs. (S13) and (S14), we have $\partial\hat{K}/\partial\tau_0^{-1} = 0$, and $\partial\hat{K}/\partial\tau_Q^{-1} = -1/T$, i.e. only large-momentum scattering is pair-breaking. Since we apply the soft cutoff here, the weight function f also depends on temperature, as shown by Eq. (S16). We have:

$$\begin{aligned} \frac{\partial f_n}{\partial T} &= - \frac{\pi|2n+1|}{\Lambda_d} f_n(1-f_n) \\ \frac{\partial\hat{K}_{m\neq n}}{\partial T} &= - \frac{\pi}{\Lambda_d} \sqrt{\frac{\Lambda}{T}} f_m f_n \left((2n+1)(1-f_n) + (2m+1)(1-f_m) \right) \left(\frac{1}{\sqrt{|n-m|+r/T}} + \frac{1}{\sqrt{n+m+1+r/T}} \right) \\ &\quad + \frac{r}{2T^2} \sqrt{\frac{\Lambda}{T}} f_m f_n \left[(|n-m|+r/T)^{-\frac{3}{2}} + (n+m+1+r/T)^{-\frac{3}{2}} \right] - \frac{\hat{K}_{mn}}{2T} \\ \frac{\partial\hat{K}_{nn}}{\partial T} &= - \frac{\hat{K}_{nn}}{2T} - \frac{\pi(2n+1)}{2T} - \frac{2\pi(2n+1)}{\Lambda_d} \sqrt{\frac{\Lambda}{T}} \frac{f_n^2(1-f_n)}{\sqrt{2n+1+r/T}} + \frac{r}{2T^2} \sqrt{\frac{\Lambda}{T}} \frac{f_n^2}{(2n+1+r/T)^{3/2}} \\ &\quad + \frac{\pi}{\Lambda_d} \sqrt{\frac{\Lambda}{T}} f_n \sum_{m\neq n} \frac{\text{sgn}(\omega_m) f_m \left(|2m+1|(1-f_m) + (2n+1)(1-f_n) \right)}{\sqrt{|n-m|+r/T}} \\ &\quad - \frac{r}{2T^2} \sqrt{\frac{\Lambda}{T}} f_n \sum_{m\neq n} \text{sgn}(\omega_m) f_m (|n-m|+r/T)^{-3/2} \end{aligned} \quad (\text{S19})$$

A. BCS Limit

As we discussed before, the BCS limit is recovered by $r \gg \Omega_c \gg \Lambda$. In this case, it is more convenient to work with the hard cutoff, $f(\omega) = \Theta(\Omega_c - |\omega|)$. As shown in Eq. (S15), the matrix elements of \hat{K} are independent of T , but the eigenvalue η still depends on T via the changes in the matrix size $N_c = \Omega_c/(2\pi T)$. Consider a reduction in the matrix size by 1, $N_c \rightarrow N_c - 1$, which means that the last row and the last column no longer take part in the determination of the eigenvalue. Then, the change in η is given by:

$$\delta N_c = -1 \quad \eta = \sum_{m,n} \hat{K}_{mn} \bar{\Delta}_m \bar{\Delta}_n \quad \sum_m \hat{K}_{nm} \bar{\Delta}_m = \eta \bar{\Delta}_n = 0 \quad (\text{S20})$$

$$\implies \delta\eta = - \sum_m \hat{K}_{mN_c} \bar{\Delta}_m \bar{\Delta}_{N_c} - \sum_m \hat{K}_{N_c m} \bar{\Delta}_m \bar{\Delta}_{N_c} + \hat{K}_{N_c N_c} (\bar{\Delta}_{N_c})^2 = \hat{K}_{N_c N_c} (\bar{\Delta}_{N_c})^2 \quad (\text{S21})$$

Therefore, we find:

$$\frac{\delta\eta}{\delta T_c} = - \frac{\Omega_c}{2\pi T^2} \frac{\delta\eta}{\delta N_c} = \frac{\Omega_c}{2\pi T^2} \hat{K}_{N_c N_c} (\bar{\Delta}_{N_c})^2 \quad (\text{S22})$$

$$\frac{dT_c}{d\tau_Q^{-1}} = - \left(\frac{d\eta}{dT_c} \right)^{-1} \frac{d\eta}{d\tau_Q^{-1}} = \frac{2\pi T}{\Omega_c} \frac{1}{\hat{K}_{N_c N_c} (\bar{\Delta}_{N_c})^2} = \frac{1}{N_c} \frac{1}{\hat{K}_{N_c N_c} (\bar{\Delta}_{N_c})^2} \quad (\text{S23})$$

Using Eq. (S15), we have $\hat{K}_{N_c N_c} = -\pi(2N_c + 1) \approx -2\pi N_c$. Furthermore, from the same equation, we have:

$$\bar{\Delta}_{N_c} = \frac{c}{\pi(N_c + \frac{1}{2})} \sqrt{\frac{\Lambda}{r}}$$

where $c = \sum_{m \leq \frac{\Omega_c}{2\pi T}} \bar{\Delta}_m$. The value of c can be obtained by normalizing the eigenvector:

$$\sum_{n=0}^{\frac{\Omega_c}{2\pi T}} \bar{\Delta}_n^2 = 1 \implies \frac{c}{\pi} \sqrt{\frac{\Lambda}{r}} = \left(\sum_n \frac{1}{(n + 1/2)^2} \right)^{-1/2}$$

Therefore:

$$\bar{\Delta}_{N_c} = \frac{1}{N_c + 1/2} \left(\sum_n \frac{1}{(n + 1/2)^2} \right)^{-1/2} \approx \frac{\sqrt{2}}{\pi N_c} \implies \frac{dT_c}{d\tau_Q^{-1}} \approx -\frac{1}{N_c} \frac{1}{2\pi N_c} \left(\frac{\pi N_c}{\sqrt{2}} \right)^2 = -\frac{\pi}{4}.$$

recovering the Abrikosov-Gor'kov universal value.

B. Quantum Critical Point

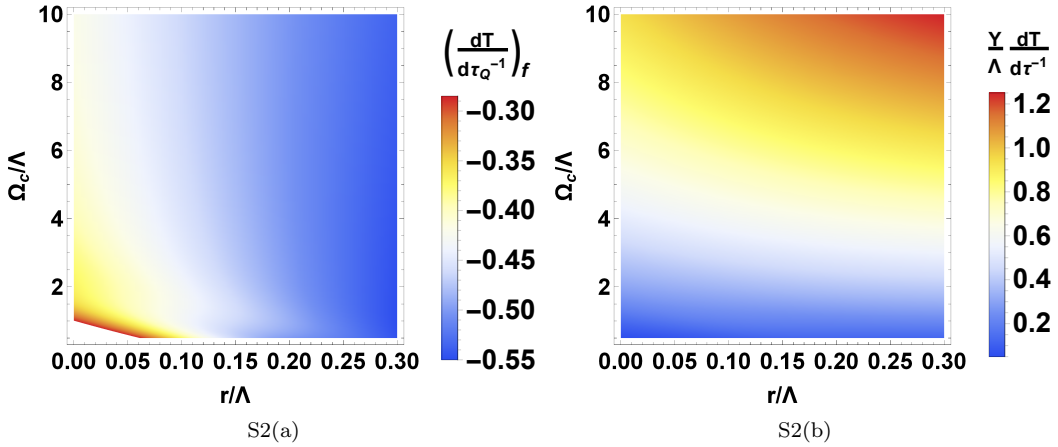


Figure S2. The suppression of T_c by disorder, $dT_c/d\tau^{-1}$, when the system is near the quantum critical point $r = 0$. In both plots, we used the hard cutoff procedure. The left panel shows the effects of the coupling of disorder to the fermions, $(dT_c/d\tau^{-1})_f$, whereas the right panel shows the effects of the coupling of disorder to the bosons, $(dT_c/d\tau^{-1})_b = (dT_c/d\tau^{-1})_{b_1} + (dT_c/d\tau^{-1})_{b_2}$.

Fig. S2(a) presents $dT_c/d\tau_Q^{-1}$ in the proximity of a QCP, revealing that in general T_c is in general more robust against disorder at the QCP ($r = 0$), especially when compared to the AG universal value $-\pi/4 \approx -0.785$. At the QCP, it is interesting to consider the case $\Omega_c \rightarrow \infty$, in which the system has only one energy scale, Λ . Using Eq. (S18) and setting $f_n = 1$ (since there is no cutoff), we find:

$$\frac{\partial \hat{K}_{nn}}{\partial T} = -\frac{\hat{K}_{nn}}{2T} - \frac{\pi(2n+1)}{2T} \quad \frac{\partial \hat{K}_{m \neq n}}{\partial T} = -\frac{\hat{K}_{mn}}{2T}$$

Therefore, since $\eta = \sum_{m,n} \bar{\Delta}_m \hat{K}_{mn} \bar{\Delta}_n = 0$, we find:

$$\left(\frac{d\eta}{dT} \right) = -\frac{\pi}{2T} \sum_{n=0}^{\infty} \bar{\Delta}_n^2 (2n+1) \implies \frac{dT_c}{d\tau_Q^{-1}} = -\frac{2}{\pi} \left(\sum_{n=0}^{\infty} \bar{\Delta}_n^2 (2n+1) \right)^{-1} \quad (\text{S24})$$

Numerical evaluation then gives $dT_c/d\tau_Q^{-1} \approx -0.43$, which is smaller than the AG universal value.

IV. COUPLING BETWEEN DISORDER AND BOSONS

A. Vertex renormalization

We first calculate the fermion-boson vertex renormalization by disorder, as shown in Fig. 4a of the main text. The vertex correction $\delta\lambda$ is given by:

$$\begin{aligned}\delta\lambda &= n_i u^2 \int \frac{d^2k}{(2\pi)^2} G_c \left(i\omega_n, \mathbf{k} - \frac{\mathbf{q}}{2} \right) G_d \left(i\omega_m, \mathbf{k} + \frac{\mathbf{q}}{2} + \mathbf{Q} \right) \\ &= n_i u^2 \int \frac{d^2k}{(2\pi)^2} \frac{1}{i\omega_n Z_n + \mathbf{v}_c \cdot \mathbf{q}/2 - \mathbf{v}_c \cdot \mathbf{k}} \frac{1}{i\omega_m Z_m - \mathbf{v}_d \cdot \mathbf{q}/2 - \mathbf{v}_d \cdot \mathbf{k}} \\ &= \frac{n_i u^2}{|\mathbf{v}_c \times \mathbf{v}_d|} \int \frac{d\epsilon_1 d\epsilon_2}{(2\pi)^2} \frac{1}{i\omega_n Z_n + \mathbf{v}_c \cdot \mathbf{q}/2 - \epsilon_1} \frac{1}{i\omega_m Z_m - \mathbf{v}_d \cdot \mathbf{q}/2 - \epsilon_2}\end{aligned}$$

where n_i is the impurity concentration and u is the impurity potential, which is related to the scattering rate by $\tau^{-1} = 2\pi n_i u^2 N_f$. Since the effect is the same for small and large momentum scattering, we do not distinguish them here. Note that in the last step, $\epsilon_1 = \mathbf{v}_c \cdot \mathbf{k}$, $\epsilon_2 = \mathbf{v}_d \cdot \mathbf{k}$. Using the result:

$$\int_{-\infty}^{\infty} \frac{dp}{ia - c - p} = \int_0^{\infty} dp \left(\frac{1}{ia - c - p} + \frac{1}{ia - c + p} \right) = \int_0^{\infty} dp \frac{2(ia - c)}{(ia - c)^2 - p^2} = -i\pi \text{sgn}(a) .$$

we obtain:

$$\delta\lambda = -\lambda \frac{n_i u^2}{4|\mathbf{v}_c \times \mathbf{v}_d|} \text{sgn}(\omega_n \omega_m) = -\lambda \frac{\text{sgn}(\omega_n \omega_m)}{8\pi N_f \tau |\mathbf{v}_c \times \mathbf{v}_d|} .$$

Note that the vertex correction depends only on the frequencies of two fermion legs. In the ladder approximation, we find the renormalized vertex λ_r

$$\lambda_r = \lambda \left(1 + \frac{\text{sgn}(\omega_n \omega_m)}{8\pi N_f \tau |\mathbf{v}_c \times \mathbf{v}_d|} \right)^{-1} = \lambda \left(1 + \frac{\text{sgn}(\omega_n \omega_m)}{2\Upsilon\tau} \right)^{-1} , \quad \Rightarrow \quad \left. \frac{d\lambda_r}{d\tau^{-1}} \right|_{\tau^{-1}=0} = -\lambda \frac{\text{sgn}(\omega_n \omega_m)}{2\Upsilon} .$$

where we defined the energy scale $\Upsilon = 4\pi N_f v_f^2 \sin\theta$. Thus, we have two different behaviors depending of whether both frequencies have the same sign (λ_+) or different signs (λ_-):

$$\lambda_{\pm} = \lambda \left(1 \pm \frac{1}{2\Upsilon\tau} \right)^{-1} , \quad \left. \frac{d\lambda_{\pm}}{d\tau^{-1}} \right|_{\tau^{-1}=0} = \mp \frac{\lambda}{2\Upsilon} \tag{S25}$$

B. Boson Self Energy Renormalization

We now calculate the renormalization of the particle-hole bubble by disorder, shown in Fig. 4b of the main text:

$$\begin{aligned}\Pi(i\Omega_m, \mathbf{q}) &= -2T \sum_n \int \frac{d^2q}{(2\pi)^2} \lambda_r \lambda G_c \left(i\omega_n, \mathbf{k} - \frac{\mathbf{q}}{2} \right) G_d \left(i\omega_n + i\Omega_m, \mathbf{k} + \frac{\mathbf{q}}{2} + \mathbf{Q} \right) \\ &= \frac{\lambda^2}{2|\mathbf{v}_c \times \mathbf{v}_d|} T \sum_n \frac{\text{sgn}(\omega_m(\omega_m + \Omega_n))}{1 + \frac{1}{2\Upsilon\tau} \text{sgn}(\omega_m(\omega_m + \Omega_n))}\end{aligned}$$

Therefore, the particle-hole bubble does not depend on \mathbf{q} . In the static limit, we find:

$$\Pi(0) = \frac{\lambda^2 \Omega_c}{2\pi |\mathbf{v}_c \times \mathbf{v}_d|} \left(1 + \frac{1}{2\Upsilon\tau} \right)^{-1}$$

Thus, since the correlation length is given by $\xi^{-2} = r_0 - \chi_0 \Pi(0)$, and using the definition $r = \frac{\xi^{-2} \gamma}{2\pi}$, we find:

$$\frac{dr}{d\tau^{-1}} = \frac{\Omega_c}{4\pi\Upsilon} \quad (\text{S26})$$

We can also calculate the correction to the Landau damping $\gamma^{-1} \equiv \chi_0 [\Pi(0) - \Pi(i\Omega_n)] / |\Omega_n|$. We find:

$$\begin{aligned} \Pi(0) - \Pi(i\Omega_n) &= \frac{\lambda^2}{2|\mathbf{v}_c \times \mathbf{v}_d|} T \sum_{m=1}^{|\Omega_n|/(2\pi T)} \left[\left(1 + \frac{1}{2\Upsilon\tau}\right)^{-1} + \left(1 - \frac{1}{2\Upsilon\tau}\right)^{-1} \right] \\ &= \frac{\lambda^2 |\Omega_n|}{4\pi |\mathbf{v}_c \times \mathbf{v}_d|} \left[\left(1 + \frac{1}{2\Upsilon\tau}\right)^{-1} + \left(1 - \frac{1}{2\Upsilon\tau}\right)^{-1} \right] \end{aligned}$$

yielding:

$$\gamma^{-1} = \frac{\lambda^2 \chi_0}{2\pi |\mathbf{v}_c \times \mathbf{v}_d|} (1 - (2\Upsilon\tau)^{-2})^{-1}, \quad \frac{d\gamma^{-1}}{d\tau^{-1}} = 0$$

Therefore, the Landau damping γ depends only quadratically on the scattering rate, and does not contribute to the leading order in τ^{-1} .

C. Contribution to the suppression rate of T_c

Using the results of the previous sections, we can rewrite the matrix elements in Eqs. (S16) as:

$$\begin{aligned} \hat{K}_{m \neq n} &= f_m f_n \sqrt{\frac{\Lambda}{T}} \left(\frac{(\lambda_+/\lambda)^2}{\sqrt{|n-m|+r/T}} + \frac{(\lambda_-/\lambda)^2}{\sqrt{n+m+1+r/T}} \right) \\ \hat{K}_{nn} &= \frac{2(\lambda_-/\lambda)^2 f_n^2}{\sqrt{2n+1+r/T}} \sqrt{\frac{\Lambda}{T}} - \pi(2n+1) - f_n \sqrt{\frac{\Lambda}{T}} \sum_{\substack{m \neq n \\ m=0}}^{N_c} f_m \left[\frac{(\lambda_+/\lambda)^2}{\sqrt{|n-m|+r/T}} - \frac{(\lambda_-/\lambda)^2}{\sqrt{n+m+1+r/T}} \right] - \frac{1}{\tau_Q T} \end{aligned}$$

While $\partial\eta/\partial T$ is the same as Eq. (S19), the term $\partial\eta/\partial\tau^{-1}$ acquires two new contributions arising from the vertex renormalization (b_1) and from the self-energy renormalization (b_2):

$$\left(\frac{\partial\eta}{\partial\tau^{-1}} \right)_b = \left(\frac{\partial\eta}{\partial\tau^{-1}} \right)_{b_1} + \left(\frac{\partial\eta}{\partial\tau^{-1}} \right)_{b_2}$$

Using Eq. (S25), we find:

$$\begin{aligned} \Upsilon \left(\frac{\partial\hat{K}_{m \neq n}}{\partial\tau^{-1}} \right)_{b_1} &= \sqrt{\frac{\Lambda}{T}} f_m f_n \left[\frac{-1}{\sqrt{|n-m|+r/T}} + \frac{1}{\sqrt{n+m+1+r/T}} \right] \\ \Upsilon \left(\frac{\partial\hat{K}_{nn}}{\partial\tau^{-1}} \right)_{b_1} &= 2f_n^2 \sqrt{\frac{\Lambda}{T}} (2n+1+r/T)^{-1/2} \\ &\quad + \sqrt{\frac{\Lambda}{T}} \sum_{\substack{m \neq n \\ m=0}}^{N_c} f_m f_n \left(\frac{1}{\sqrt{|n-m|+r/T}} + \frac{1}{\sqrt{n+m+1+r/T}} \right) \end{aligned}$$

Using Eq. (S26) yields:

$$\begin{aligned}
\Upsilon \left(\frac{\partial \hat{K}_{m \neq n}}{\partial \tau^{-1}} \right)_{b_2} &= -f_m f_n \frac{\Omega_c}{8\pi T} \sqrt{\frac{\Lambda}{T}} \left[(|n-m| + r/T)^{-\frac{3}{2}} + (n+m+1 + r/T)^{-\frac{3}{2}} \right] \\
\Upsilon \left(\frac{\partial \hat{K}_{nn}}{\partial \tau^{-1}} \right)_{b_2} &= -2f_n^2 \frac{\Omega_c}{8\pi T} \sqrt{\frac{\Lambda}{T}} (2n+1 + r/T)^{-\frac{3}{2}} \\
&\quad + \frac{\Omega_c}{8\pi T} \sqrt{\frac{\Lambda}{T}} \sum_{\substack{m \neq n \\ m=0}}^{N_c} f_m f_n \left[(|n-m| + r/T)^{-\frac{3}{2}} - (n+m+1 + r/T)^{-\frac{3}{2}} \right]
\end{aligned}$$

Fig. S2(b) shows $dT_c/d\tau^{-1}$ due to the coupling of disorder to the bosons, near the QCP. Clearly, we find in general that these effects enhance T_c . To understand this behavior, we focus on the case where the system is at the QCP, $r=0$, and apply the hard cutoff procedure for $N_c \gg 1$. In this case, the expressions above simplify to:

$$\begin{aligned}
\Upsilon \left(\frac{\partial K_{mn}}{\partial \tau^{-1}} \right)_{b_1} &= \sqrt{\frac{\Lambda}{T}} \left[2\zeta \left(\frac{1}{2}, 1 \right) - \zeta \left(\frac{1}{2}, N_c - n \right) - \zeta \left(\frac{1}{2}, N_c + n \right) \right] \delta_{mn} - \sqrt{\frac{\Lambda}{T}} \left[\frac{1 - \delta_{mn}}{\sqrt{|m-n|}} - \frac{1}{\sqrt{m+n+1}} \right] \\
\Upsilon \left(\frac{\partial \hat{K}_{mn}}{\partial \tau^{-1}} \right)_{b_2} &= \frac{\Omega_c}{4\pi T} \sqrt{\frac{\Lambda}{T}} \left\{ \left[\zeta \left(\frac{3}{2}, 1 \right) - \zeta \left(\frac{3}{2}, n+1 \right) \right] \delta_{mn} - \frac{1}{2} \left[\frac{1 - \delta_{mn}}{|m-n|^{3/2}} + \frac{1}{(m+n+1)^{3/2}} \right] \right\}
\end{aligned}$$

where $\zeta(a, x)$ is the Hurwitz zeta function. We first focus on the b_1 contribution above. In the limit $N_c \gg 1$, the off-diagonal term is much smaller than the diagonal one. Consequently, the change in the eigenvalue is given by:

$$\Upsilon \sqrt{\frac{T}{\Lambda}} \left(\frac{d\eta}{d\tau^{-1}} \right)_{b_1} = 2 \sum_{n=0}^{N_c} \bar{\Delta}_n^2 \left(\sqrt{N_c - n} + \sqrt{N_c + n} \right)$$

where the eigenvectors are normalized, $\sum_n \bar{\Delta}_n^2 = 1$. As discussed in the solution of the clean case, $\bar{\Delta}_{n \geq n_0} \approx A n^{-3/2}$ for $1 \ll n_0 \ll N_c$, with $A > 0$. Thus, we obtain:

$$\begin{aligned}
\Upsilon \sqrt{\frac{T}{\Lambda}} \left(\frac{d\eta}{d\tau^{-1}} \right)_{b_1} &\approx 4\sqrt{N_c} \sum_{n=0}^{n_0} \bar{\Delta}_n^2 + 2A^2 \int_{n_0}^{N_c} dn \left(\frac{\sqrt{N_c - n} + \sqrt{N_c + n}}{n^3} \right) \\
&\approx 4\sqrt{N_c} \sum_{n=0}^{n_0} \bar{\Delta}_n^2 + \frac{2A^2 \sqrt{N_c}}{n_0^2}
\end{aligned}$$

yielding:

$$\Upsilon \left(\frac{d\eta}{d\tau^{-1}} \right)_{b_1} \approx \frac{8}{\sqrt{2\pi}} \sqrt{\frac{\Omega_c}{\Lambda}}. \quad (\text{S27})$$

where we used the clean limit result $T_c \approx \Lambda/2$. Therefore, T_c actually increases due to the dressing of the fermion-boson vertex by disorder. To evaluate the change in T_c due to this effect, we use Eq. (S24):

$$-\left(\frac{d\eta}{dT} \right) = -\frac{\pi}{2T} \sum_{n=0}^{\infty} \bar{\Delta}_n^2 (2n+1) \approx \frac{1.6\pi}{\Lambda} \quad (\text{S28})$$

where the last step was obtained by the numerical solution of the clean system at the QCP. Therefore, we obtain:

$$\frac{\Upsilon}{\Lambda} \left(\frac{dT_c}{d\tau^{-1}} \right)_{b_1} \approx 0.6 \sqrt{\frac{\Omega_c}{\Lambda}} \quad (\text{S29})$$

In Fig. S3(a), the numerical solution is compared to this approximate analytical expression, yielding very good agreement.

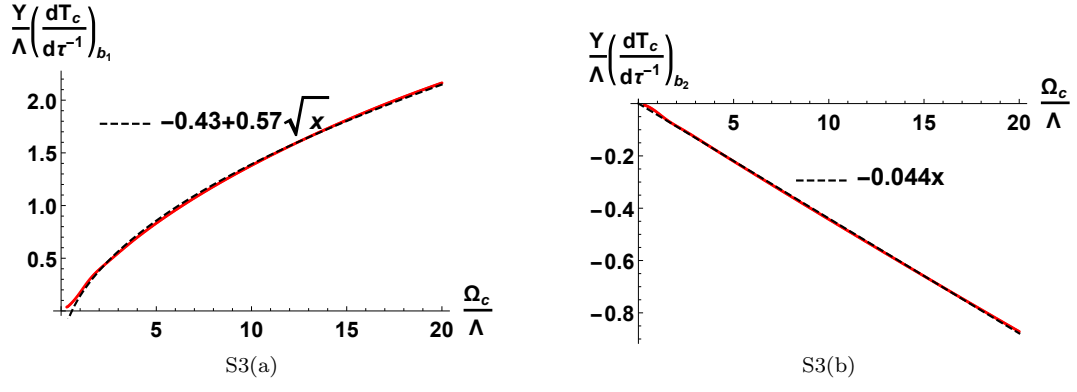


Figure S3. Contribution to the suppression rate $(dT_c/d\tau^{-1})$ arising from the impurity dressing of (a) the fermion-boson coupling and (b) the bosonic self-energy.

As for the contribution arising from the bosonic self-energy, we find:

$$\Upsilon \sqrt{\frac{T}{\Lambda}} \frac{4\pi T}{\Omega_c} \left(\frac{d\eta}{d\tau^{-1}} \right)_{b_2} = \sum_n \bar{\Delta}_n^2 \left[\zeta \left(\frac{3}{2}, 1 \right) - \zeta \left(\frac{3}{2}, n+1 \right) \right] - \frac{1}{2} \sum_{m,n} \bar{\Delta}_m \bar{\Delta}_n \left[\frac{1 - \delta_{mn}}{|m-n|^{3/2}} + \frac{1}{(m+n+1)^{3/2}} \right]$$

Using the numerical solution of the clean system at the QCP, we find for the right-hand side of the equation:

$$\Upsilon \sqrt{\frac{T}{\Lambda}} \frac{4\pi T}{\Omega_c} \left(\frac{d\eta}{d\tau^{-1}} \right)_{b_2} \approx -1$$

yielding:

$$\frac{\Upsilon}{\Lambda} \left(\frac{dT_c}{d\tau^{-1}} \right)_{b_2} \approx -0.045 \frac{\Omega_c}{\Lambda} \quad (\text{S30})$$

This behavior is also consistently captured by the numerical solution presented in Fig. S3(b).